



iJRASET

International Journal For Research in
Applied Science and Engineering Technology



INTERNATIONAL JOURNAL FOR RESEARCH

IN APPLIED SCIENCE & ENGINEERING TECHNOLOGY

Volume: 5 Issue: VIII Month of publication: August 2017

DOI: <http://doi.org/10.22214/ijraset.2017.8164>

www.ijraset.com

Call: ☎ 08813907089

E-mail ID: ijraset@gmail.com

MHD Mixed Convection Nanofluid Flow through a Stratified Radiative Stretching Cylinder

Srinivas Maripala¹, Kishan Naikoti²

¹Department of Mathematics, SNIST, Hyderabad, 501301.

²Department of Mathematics, Osmania University, Hyderabad, 500007.

Abstract: In this paper, is study the mixed convection nanofluid flow along a stretching cylinder embedded in a thermally stratified medium are numerically analyzed, with the thermal radiation effects. The governing boundary layer equations of continuity, momentum, energy and concentration are transformed into a set of ordinary differential equations with the help of suitable local similarity transformations. The coupled non-linear ordinary differential equations are solved by the implicit finite difference method along with the Thomas algorithm. The effect of various material parameters such as buoyancy parameter, solutal buoyancy parameter, Prandtl number, radiation parameter, Schmidt number, curvature parameter, magnetic parameter, stratification parameter, Brownian motion parameter and thermophoresis parameter on the velocity, temperature and concentration profiles are presented in graphs. Physical quantities such as skin friction coefficient, Nusselt number and Sherwood number are also computed.

Keywords: Nanofluid, thermal radiation, thermal stratification, mixed convection, Mass transfer; stretching cylinder.

I. INTRODUCTION

Nanofluid is a fluid containing nanometer-sized particles, called nanoparticles. The term nanofluid has been first proposed by Choi [1], has been verified that addition of nanoparticles in conventional base fluids appreciably enhanced the thermal conductivity. Heat transfer has enormous applications in many manufacturing processes for example, in microelectronics, fuel cells, hybrid-powered engines nuclear reactors, transportations, biomedicine/pharmaceutical processes and pasteurization of food. In these processes, heat transfer takes place through some heat transfer devices; such as heat exchangers, evaporators, condensers and heat sinks. Increasing the heat transfer efficiency of these devices is desirable to minimize the space. Further in most of the heat transfer systems the working fluid is circulated by a pump, so the associated power consumption should be minimized [2]. A variety of nuclear reactor designs featured by enhanced safety and improved economics are being proposed by the nuclear power industry around the world to more realistically solve the future energy supply shortfall. In order to secure safety and economics, nanofluid coolants exhibiting improve thermal performance are being considered as a new key technology [3]. Thermal conductivity of nanofluids depends on many factors such as particle volume fraction, particle material, particle size and shape, base fluid material and temperature [2]. The study of boundary layer flow and heat transfer over an exponentially stretching cylinder has attracted many researchers due to its applications in fiber technology, flow meter design, piping and casting systems etc. Lin and Shih [4], [5] analyzed the laminar boundary layer and heat transfer along horizontally and vertically moving cylinders with constant velocity and found that the similarity solutions could not be obtained due to the curvature effect of the cylinder. Wang [6] investigated the steady flow of a viscous and incompressible fluid outside a stretching hollow cylinder in an ambient fluid at rest. Ishak et al. [7] studied the flow and heat transfer of an incompressible electrically conducted viscous fluid outside of a stretching cylinder in the presence of a constant transverse magnetic field. Elbashbeshy et al. [8] studied laminar boundary layer flow of an incompressible viscous fluid along a stretching horizontal cylinder embedded in a porous medium in the presence of a heat source or sink with suction/injection. Nazar et al. [9] analyzed mixed convection of nanofluids from a horizontal circular cylinder embedded in a porous medium. In the work of Nazar et al. [9], the effect of copper, alumina and titanium oxide nanoparticles is evaluated. In the study of the effect of porosity and the thermal conductivity of porous medium on the effective thermal conductivity of the representative elementary. Srinivas Maripala and Kishan Naikoti [10], studied the forced convection in unsteady magneto-hydrodynamic boundary layer flow of a nanofluid over a permeable shrinking sheet in the presence of thermal radiation and chemical reaction

II. MATHEMATICAL ANALYSIS

A steady axis-symmetric mixed convection nanofluid flow of an incompressible viscous radiating fluid along a stretching cylinder embedded in a thermally stratified nanofluid-saturated medium of variable ambient temperature $T_\infty(x)$, where $T_w(x) > T_\infty(x)$

(heated surface), is considered. UNiform magnetic field intensity B_0 acts the radial direction, it is assumed that the effect of the induced magnetic field is negligible, which is valid when the magnetic Reynolds number is small. The fluid is considered to be a gray, absorbing emitting radiation but non-scattering medium. The flow model and coordinate system are depicted.

The temperature and concentration of nanofluid outside the boundary layer are constant except that the influence of the density variation with temperature and concentration in the body force term (Boussinesq's approximation). Under the above assumptions the conservation equations of mass, momentum, energy and diffusion that govern the flow field are

$$\frac{\partial(ru)}{\partial x} + \frac{\partial(rv)}{\partial y} = 0 \quad (1)$$

$$u \frac{\partial u}{\partial x} + v \frac{\partial u}{\partial r} = \frac{\nu}{r} \frac{\partial}{\partial r} \left(r \frac{\partial u}{\partial r} \right) + g\beta(T - T_\infty) + g\beta^*(C - C_\infty) - \frac{\sigma B_0^2}{\rho} u \quad (2)$$

$$u \frac{\partial T}{\partial x} + v \frac{\partial T}{\partial y} = \frac{k}{\rho C_p} \frac{1}{r} \frac{\partial}{\partial r} \left(r \frac{\partial T}{\partial r} \right) - \frac{1}{\rho C_p} \frac{1}{r} \frac{\partial(rq_r)}{\partial r} + \tau \left[D_B \frac{\partial C}{\partial r} \frac{\partial T}{\partial r} + \frac{D_T}{T_\infty} \left(\frac{\partial T}{\partial r} \right)^2 \right] \quad (3)$$

$$u \frac{\partial C}{\partial x} + v \frac{\partial C}{\partial r} = \frac{D}{r} \frac{\partial}{\partial r} \left(r \frac{\partial C}{\partial r} \right) + \frac{D_T}{T_\infty} \frac{1}{r} \frac{\partial}{\partial r} \left(r \frac{\partial T}{\partial r} \right) \quad (4)$$

where u and v are the components of velocity in the x and r directions, respectively, $\nu = \mu/\rho$ is the kinematic viscosity, ρ is the fluid density, μ is the coefficient of fluid viscosity, k is the thermal conductivity of the fluid T is the fluid temperature, σ is the electrical conductivity of nanofluid and B_0 is the strength of the uniform magnetic field, D_B is the Brownian diffusion coefficient, D_T is the thermophoresis diffusion coefficient. τ is the ratio between the effective heat capacity of the nanoparticles (ρ_{C_p}) and heat capacity of the nanofluid ($\rho_{C_{nf}}$), i.e. $\tau = \rho_{C_p}/\rho_{C_{nf}}$. It is assumed that the convecting fluid and the medium are in local thermodynamic equilibrium.

The boundary conditions for the velocity, temperature and concentration of the problem are

$$u = U(x), v = 0, T = T_w(x), C = C_w \quad \text{at } r = R \quad (5)$$

$$u \rightarrow 0, T \rightarrow T_\infty, C \rightarrow C_\infty \quad \text{as } r \rightarrow \infty$$

where R is the radius of the cylinder, $U(x) = U_0(x)/L$ is the stretching velocity, $T_w(x) = T_0 + b(x/L)$ is the prescribed surface temperature and $T_\infty(x) = T_0 + c(x/L)$ is the variable ambient temperature. Further, U_0 is the reference velocity, T_0 - the reference temperature and L - the characteristic length. By using the Rosseland approximation (Brewster [11]), the radiative heat flux is given by

$$q_r = (-4\sigma_s/3k_e) \frac{\partial T^4}{\partial r} \quad (6)$$

where σ_s is the Stephen Boltzmann constant and k_e - the mean absorption coefficient. It should be noted that by using the Rosseland approximation, the present analysis is limited to optically thick fluids. If the temperature differences within the flow are sufficiently small, then equation (5) can be linearized by expanding T^4 into the Taylor series about T_∞ , which after neglecting higher order terms takes the form

$$T^4 \cong 4T_\infty^3 T - 3T_\infty^4 \quad (7)$$

Invoking equations (6) and (7), equation (3) can be modified as

$$u \frac{\partial T}{\partial x} + v \frac{\partial T}{\partial y} = \frac{k}{\rho C_p} \frac{1}{r} \frac{\partial}{\partial r} \left(r \frac{\partial T}{\partial r} \right) + \frac{16\sigma_s T_\infty^3}{3\rho C_p k_e} \frac{1}{r} \frac{\partial}{\partial r} \left(r \frac{\partial T}{\partial r} \right) + \tau \left[D_B \frac{\partial C}{\partial r} \frac{\partial T}{\partial r} + \frac{D_T}{T_\infty} \left(\frac{\partial T}{\partial r} \right)^2 \right] \quad (8)$$

To get similarity solutions of equations (1) - (4) subject to the boundary conditions (5), we introduce the following similarity transformation:

$$\eta = \frac{r^2 - R^2}{2R} \sqrt{\frac{U}{\nu x}}, \psi = (U\nu x)^{\frac{1}{2}} R f(\eta), \theta(\eta) = \frac{T - T_\infty}{T_w - T_0}, \varphi(\eta) = \frac{C - C_\infty}{C_w - C_\infty}, M = \frac{\sigma B_0^2 a^2}{4\nu\rho} \quad (9)$$

$$S = \frac{c}{b}, \lambda = \frac{g\beta L b}{U_0^2}, Nb = \frac{g\beta^* L^2 (C_w - C_\infty)}{U_0^2}, Nr = \frac{k_e k}{4\sigma T_\infty^3}, A = \sqrt{\frac{\nu L}{U_0 R^2}} \quad (10)$$

where ψ is the stream function and the velocity components are defined as, $u = \frac{1}{r} \frac{\partial \psi}{\partial r}$, $v = -\frac{1}{r} \frac{\partial \psi}{\partial x}$, which identically satisfies the continuity equation (1).

Using the above similarity transformations, equations (2) - (4) reduce to

$$(1 + 2A\eta)f''' + 2Af'' + ff'' - f'^2 + \lambda\theta + \delta\varphi - Mf' = 0 \quad (11)$$

$$\left(1 + \frac{4}{3Nr}\right) \{ (1 + 2A\eta)\theta'' + 2A\theta' \} + Pr(\theta' - f'\theta - f'S) + Pr\eta\theta'(Nb\varphi' + Nt\theta') = 0 \quad (12)$$

$$(1 + 2A\eta)\varphi'' + 2A\varphi' + Scf\varphi' + \frac{Nt}{Nb}(\eta\theta'' + \theta') = 0 \quad (13)$$

The corresponding boundary conditions are

$$f' = 1, f = 0, \theta = 1 - S, \varphi = 1 \text{ at } \eta = 0 \quad (14)$$

$$f' \rightarrow 0, \theta \rightarrow 0, \varphi \rightarrow 0 \quad \text{as } \eta \rightarrow \infty$$

where prime denotes differentiation with respect to η , S is the stratification parameter, λ - the mixed convection parameter, δ - the volumetric concentration expansion, Nr - the radiation parameter, A - the curvature parameter, Pr - Prandtl number, Le - Lewis number, Nb - Brownian motion parameter and Nt - thermophoresis parameter. We note that $S = 0$ is for an unstratified environment and $A = 0$ is for a flat plate. From technological point of view, it is of interest to calculate the shear stress, heat and mass fluxes which is given by

$$\tau_w = \mu \left(\frac{\partial u}{\partial r} \right)_{r=R} = \frac{\mu U_0 x}{L} \sqrt{\frac{U_0}{\nu L}} f''(0)$$

$$q_w = -k \left(\frac{\partial T}{\partial r} \right)_{r=R} = \frac{-k b x}{L} \sqrt{\frac{U_0}{\nu L}} \theta'(0) \quad \text{and}$$

$$M_w = -D \left(\frac{\partial C}{\partial r} \right)_{r=R} = -D (C_w - C_\infty) \sqrt{\frac{U_0}{\nu L}} \varphi'(0)$$

In terms of non-dimensional quantities, the skin friction coefficient, Nusselt number and Sherwood number are given by

$$C_f = \frac{\tau_w}{\rho U_0^2 / 2} \Rightarrow \frac{1}{2} C_f Re_x^{1/2} = f''(0)$$

$$Nu_x = \frac{L q_w}{k b} \Rightarrow Nu_x Re_x^{1/2} = -\theta'(0) \quad \text{and}$$

$$Sh_x = \frac{x M_w}{D (C_w - C_\infty)} \Rightarrow \frac{Sh_x}{Re_x^{1/2}} = -\varphi'(0)$$

The governing boundary layer and thermal layer (11)-(13) with boundary conditions (14)

are coupled non-linear ordinary differential equations. Applying the Quasi-linearization technique to the non-linear equation (11) and (12). Here the step size taken as $h = 0.05$ is obtained the numerical solution and solved the algebraic system of equations by using an implicit finite difference scheme of Crank-Nickolson method with Thomas algorithm and five decimal accuracy is the criterion for convergence.

Table-I: Values of $f''(0)$, $\theta'(0)$ and $-\varphi'(0)$ for different values of Nt , Nb , Pr and A with $\lambda = 0.1, \delta = 0.1, Nr = 1.0, S = 0.0, Sc = 0.1$.

		$f''(0)$	$\theta'(0)$	$-\varphi'(0)$
Nt	0.3	0.42187	-0.43170	2.81962
	0.5	0.43297	-0.37333	2.96866
	1.0	0.45462	-0.29950	3.16633
Nb	0.3	0.42187	-0.43170	2.81962
	0.5	0.43345	-0.3191	2.93226
	1.0	0.44561	-0.2101	2.98209
Pr	0.72	0.42187	-0.43170	2.81962
	2.0	0.42380	-0.38250	2.25579
	3.0	0.42545	-0.29450	2.38523
A	1.0	0.60140	-1.61724	0.83258
	3.0	0.41344	-0.41314	2.01824
	5.0	1.67862	-0.50174	2.12550

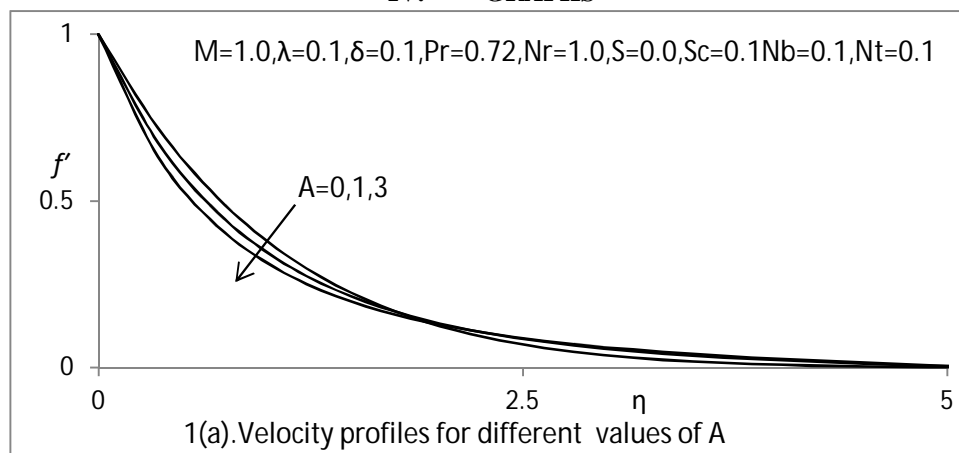
III. RESULTS

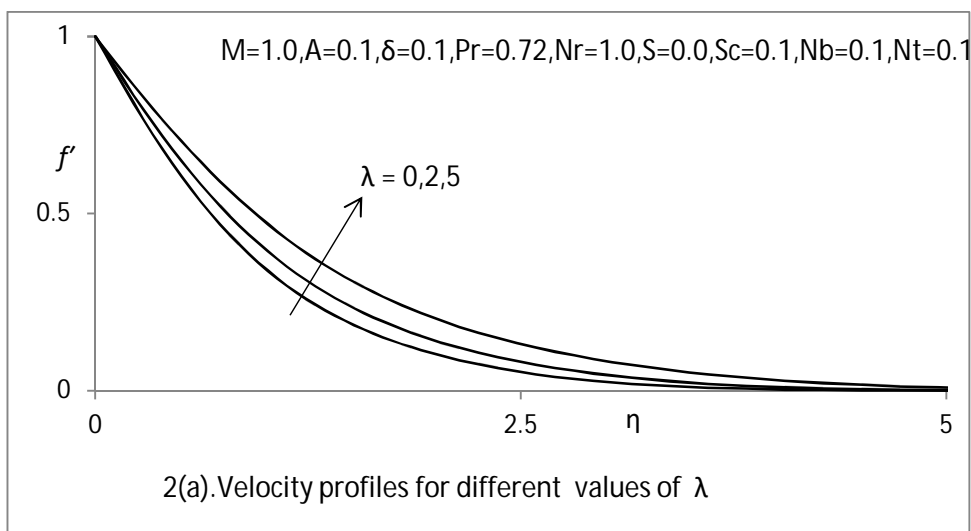
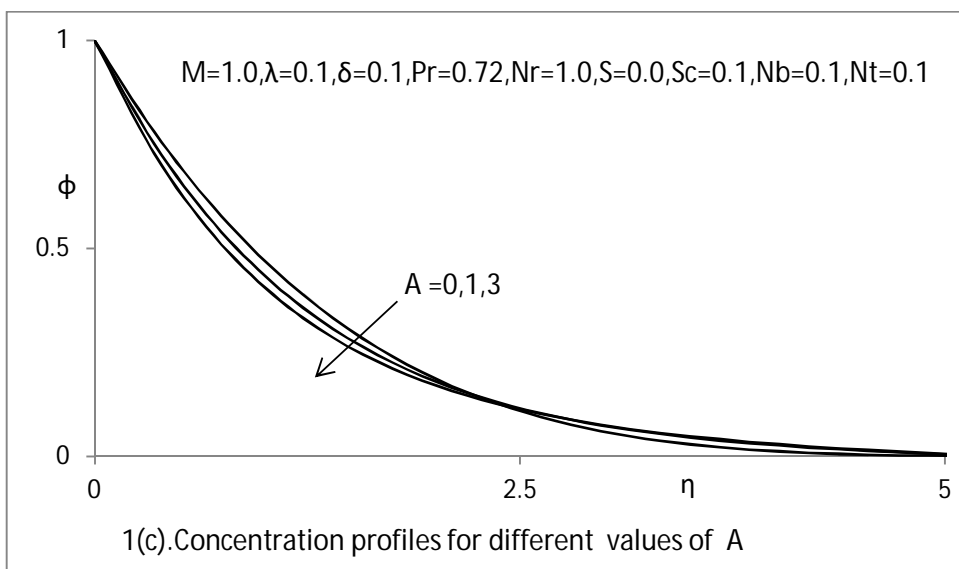
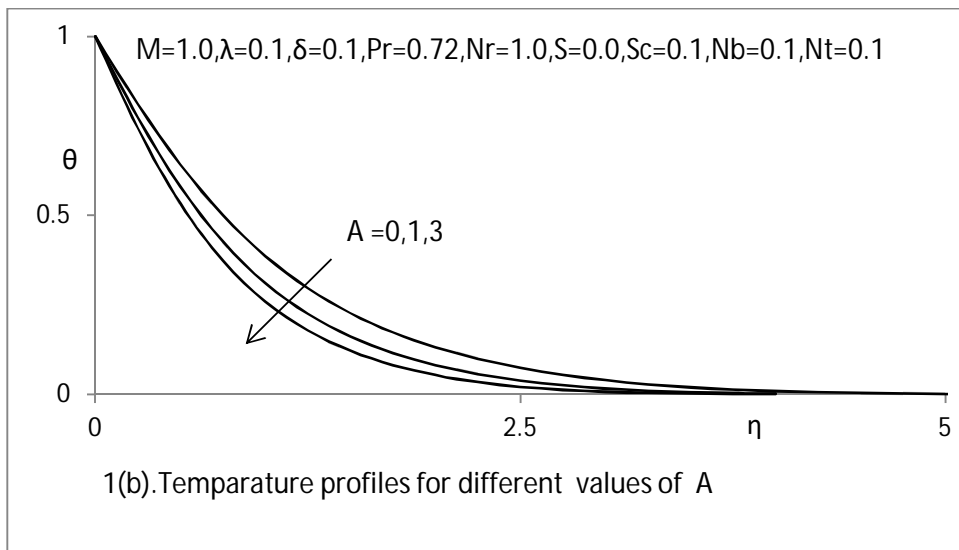
The non-linear boundary value problem given by equations (11) –(13) and boundary conditions (14) has been solved by using the implicit finite difference scheme of Crank-Nickolson type has been employed. The system of equations are reduced to tri-diagonal system of equations which are solved by the Thomas algorithm. The results have been carried out for various flow parameters such as buoyancy parameter λ , solutal buoyancy parameter δ , Prandtl number Pr , Radiation parameter Nr , Schmidt number Sc , curvature parameter A , magnetic parameter M , stratification parameter S , Brownian motion parameter Nb and thermophoresis parameter Nt on velocity, temperature and concentration fields are presented graphically in Figs.1 - 10. Here the value of Pr is chosen as 0.71, which corresponds to air. The other parameters are chosen arbitrarily. Table-I presents the numerical values of the skin friction

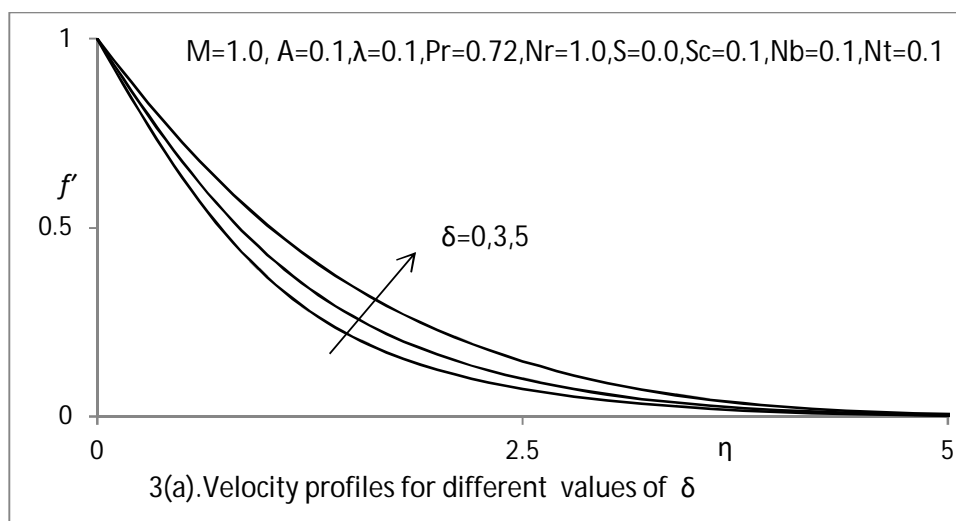
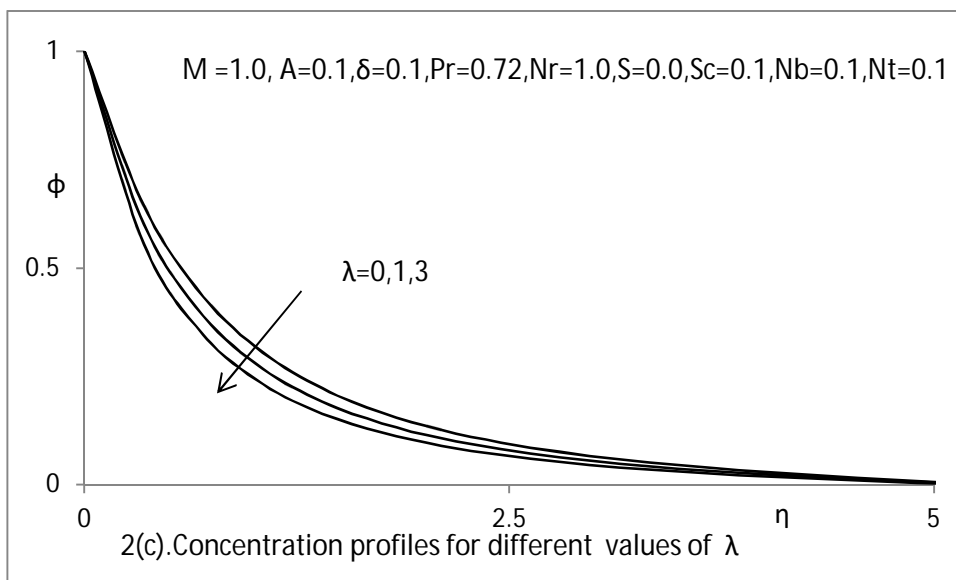
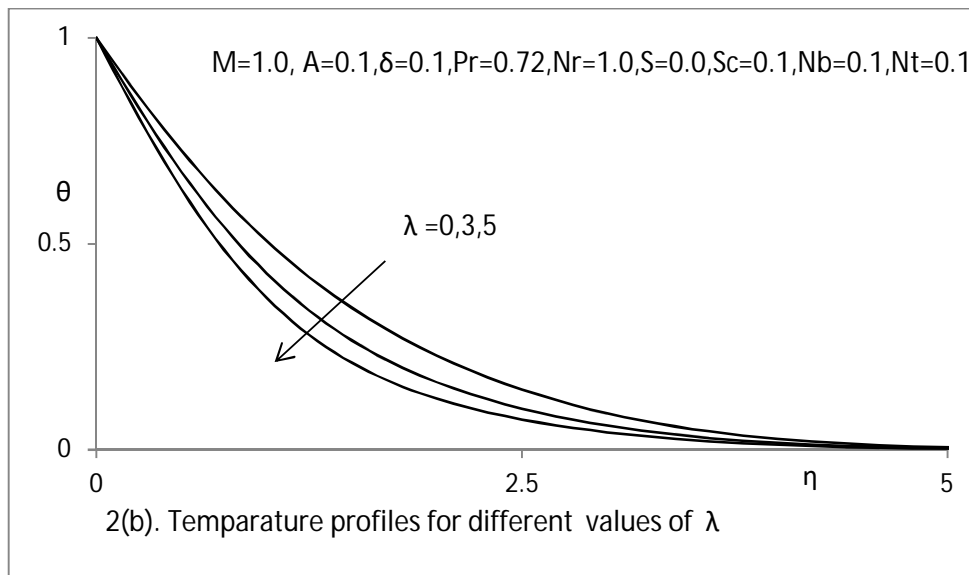
coefficient, Nusselt number and Sherwood number for various values of governing parameters. Table-I, it is observed that the skin friction coefficient, Nusselt number and Sherwood numbers are increased for both the cases Brownian motion parameter Nb and thermophoresis parameter Nt increases. The Prandtl number Pr decreases the values of skin friction coefficient $f''(0)$, Nusselt number $-\theta'(0)$ and the Sherwood number $-\phi'(0)$ values increases. The curvature parameter A decrease the values of Nusselt number and Sherwood number and increases the values of skin friction parameter.

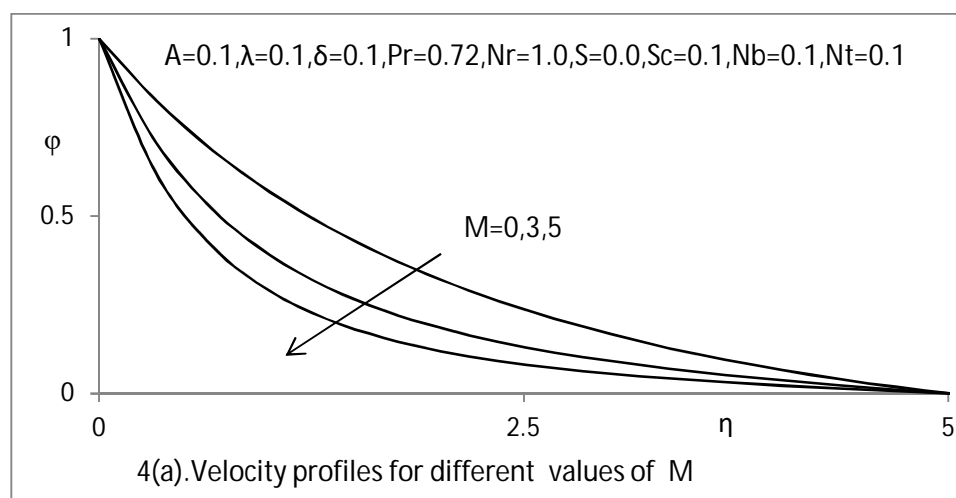
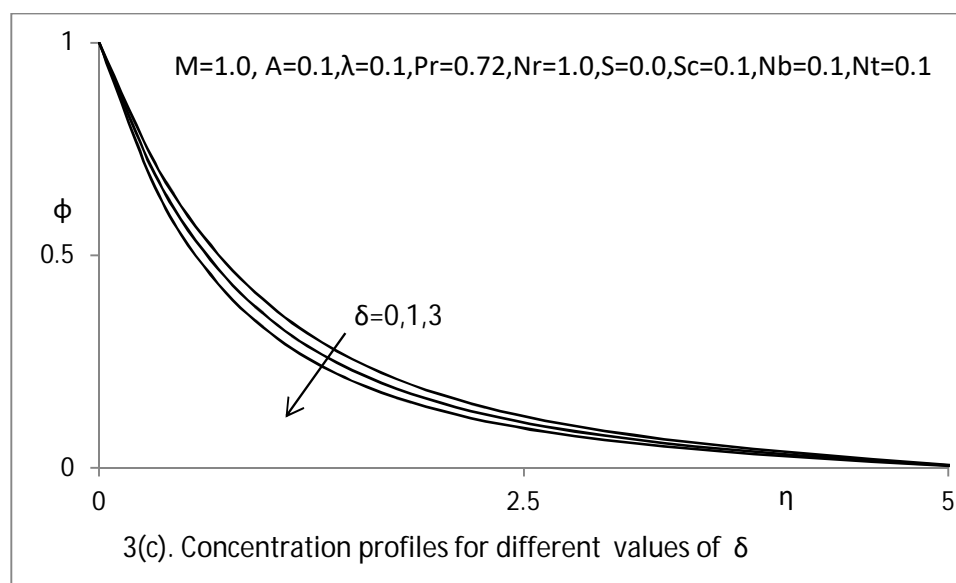
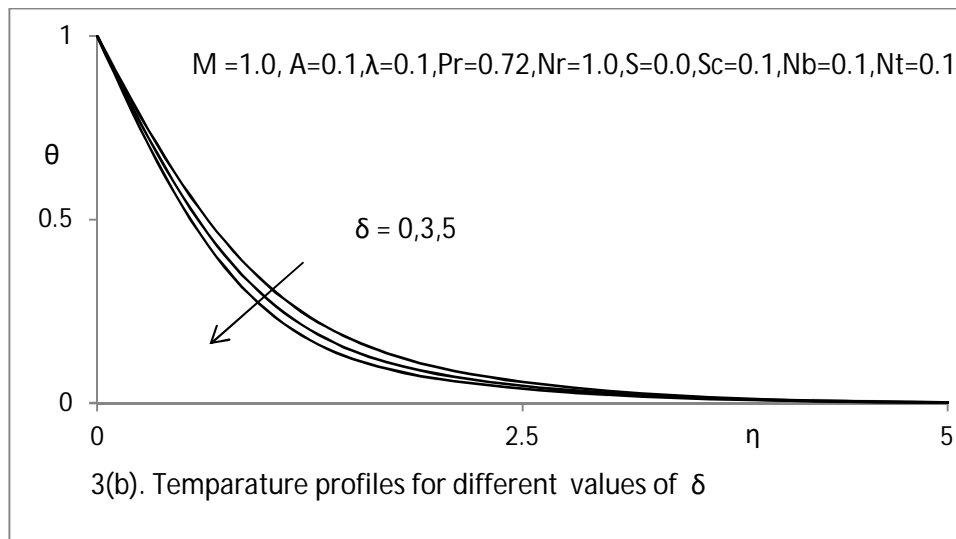
Figures 1(a) - (c) represent the effect of curvature parameter A on the velocity, temperature and concentration. Physically $A = 0$ signifies the cylinder's outer surface behaves like a flat surface. It means as $A \rightarrow 1$, the viscosity effect reduces due to contact area of surface with fluid tends to the tangential position. From Figure1 (a), it is noticed that the effect of curvature parameter A on the velocity field. In this case, nearer to the boundary layer, the velocity profiles decreases and reverse phenomenon observed far away from the boundary layer. Similar trend is observed for both the temperature and concentration i.e., initially both temperature and concentration and then they increase. The thermal buoyancy parameter λ effects are shown in Figure 2(a)–(c). The effect of the thermal buoyancy parameter λ on the velocity is presented in Fig.2(a). It is the fact that the positive buoyancy force acts like a favorable pressure gradient and hence accelerates the velocity of the fluid in the boundary layer. This results in higher velocity as λ increases. Fig.2(b). illustrates the temperature profiles for different values of the thermal buoyancy parameter. It is observed that as the thermal buoyancy parameter increases, the temperature decreases. The concentration profiles for different values of the thermal buoyancy parameter λ are depicted in Fig. 2(c). It is noticed that the concentration decreases, as the thermal buoyancy parameter increases. The effect of the solutal buoyancy parameter δ on the velocity, temperature and concentration is shown in Figs.3 (a) – (c). With an increase in the solutal buoyancy parameter δ , the velocity increases while the temperature and the concentration decrease. It is observed from Figure 4(a) - (c), that an increase in magnetic parameter M leads to a decrease in velocity profiles. The velocity boundary layer thickness becomes thinner as M increases. This is due to the fact that applications of magnetic field to an electrically conductivity fluid produce a drag-like force called Lorentz force. This force causes reduction in the fluid velocity. The thermal boundary layer thickness increases with the increasing the magnetic parameter M has shown in figure 4(b). The reason for this behavior is that the Lorentz force increases the temperature. The concentration profiles are increased with the increase of magnetic field parameter M is observed from Figure 4(c). The thermophoresis parameter Nt effects on Temperature and concentration profiles are illustrated through the graphs 5(a)-(b). It is observed that the thermophoresis parameter Nt leads to increase the temperature profiles and nanoparticle concentration. The effect of Brownian motion parameter Nb is to display on temperature and concentration profiles in figure 6(a) - 6(b). It is noticed that the temperature in the boundary layer increases and the nanoparticle concentration decreases with increase of Brownian motion parameter Nb . The temperature profiles for different values of the radiation parameter Nr are illustrated in Fig.7. It is noticed that as the radiation parameter Nr increases, the temperature decreases. The influence of the stratification parameter S on temperature profiles is shown in Fig.8. The thermal boundary layer thickness decreases with an increase in the stratification parameter S . Due to stratification, the temperature in the boundary layer decreases.

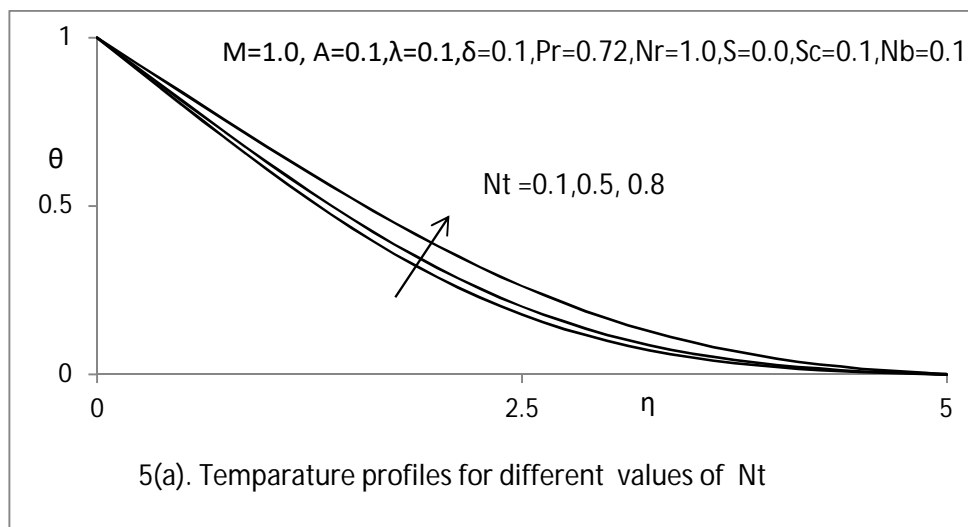
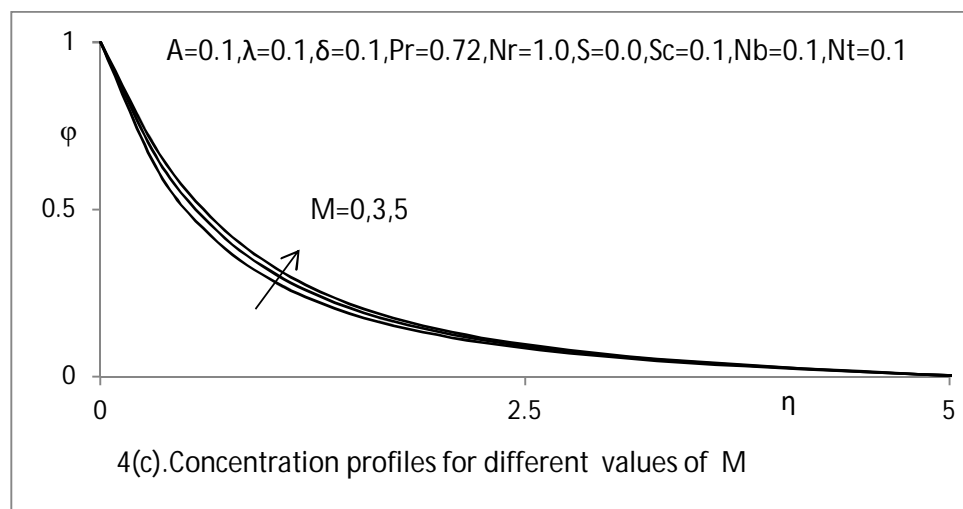
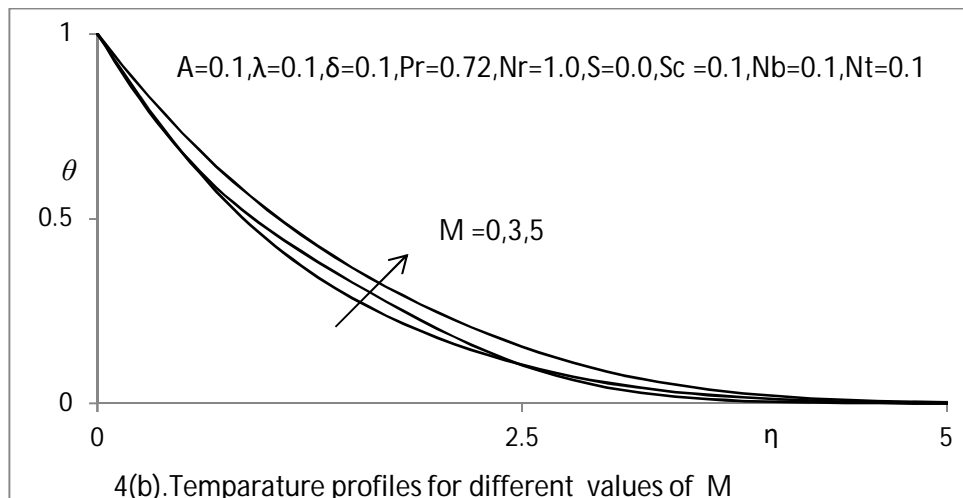
IV. GRAPHS

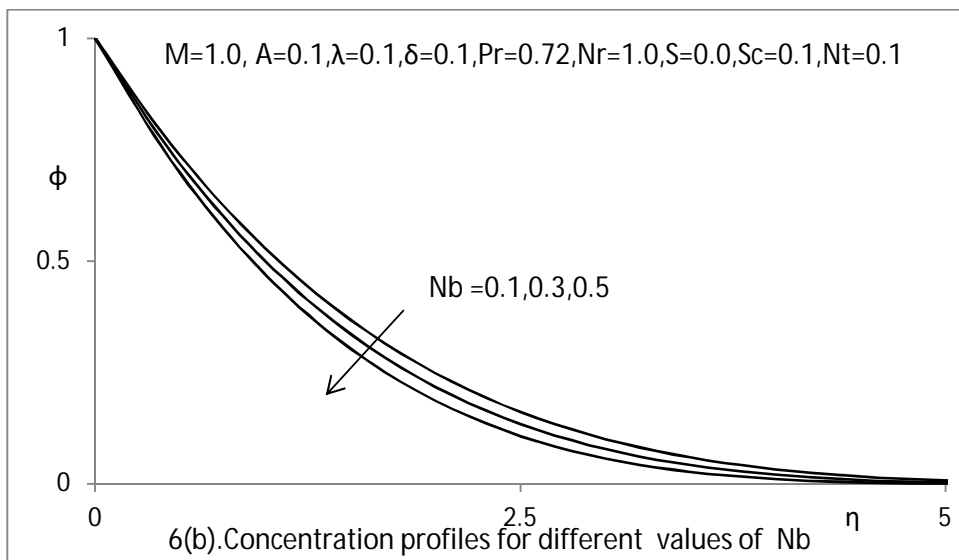
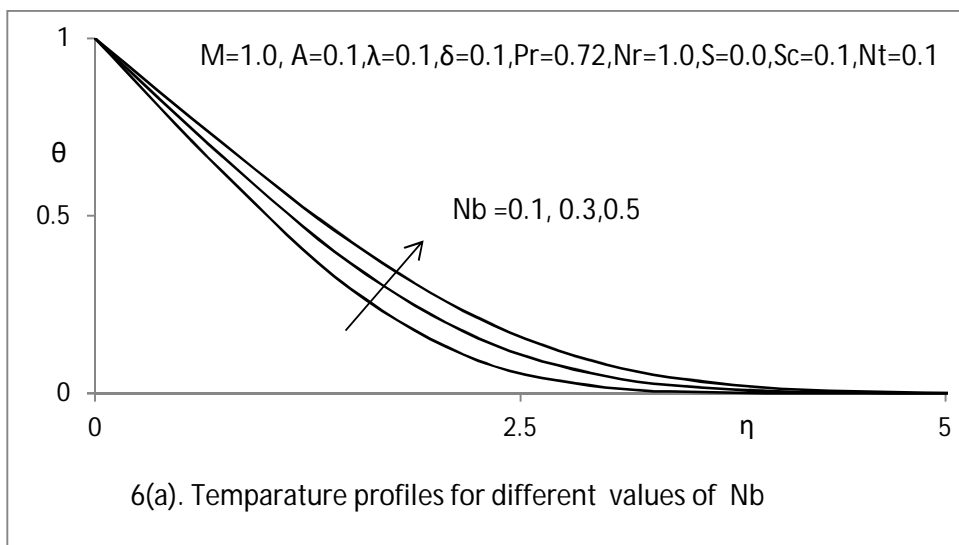
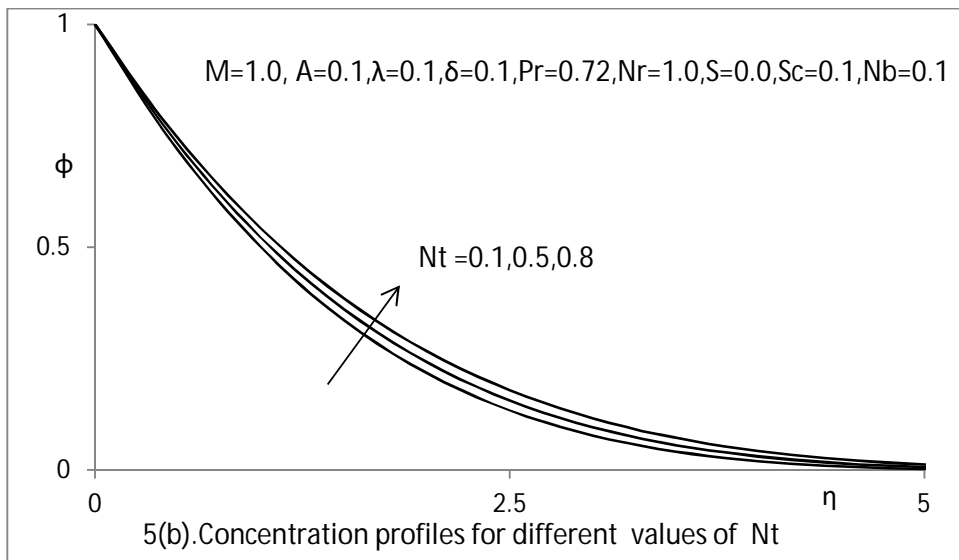


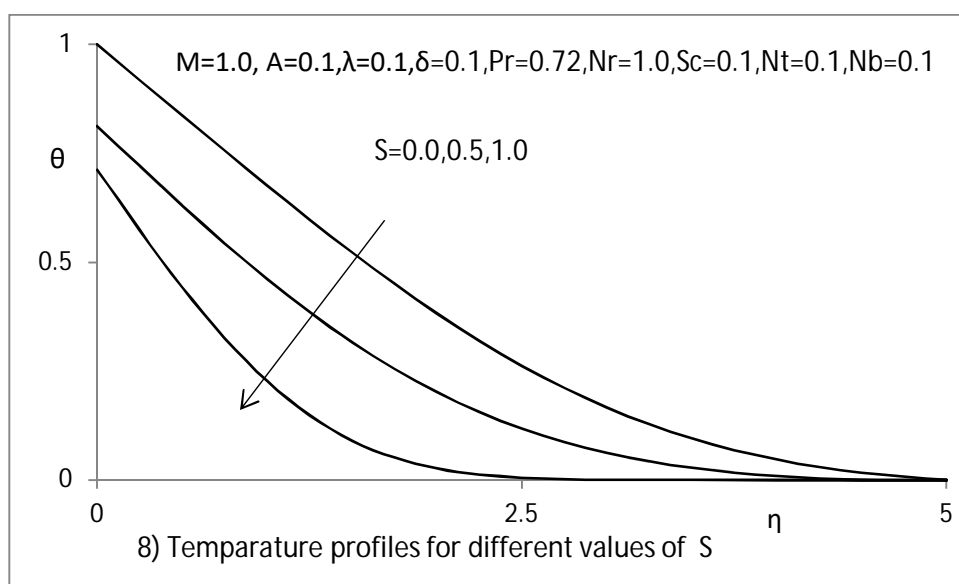
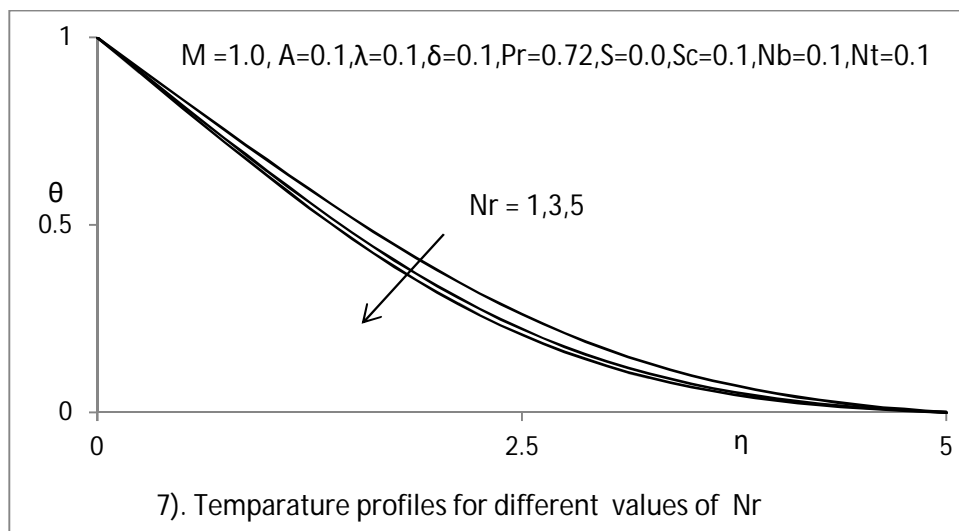












REFERENCES

- [1] Choi SUS (1995) The Proceedings of the ASME. IntMechEng Congress and Exposition, San Francisco, USA, ASME, FED 231/MD 66:99–105.
- [2] Ozernic S, Kakac S, Yazicioglu AG (2012) Enhanced thermal conductivity of nano fluids: A State of the art review, Microfluid. Nanofluid, 8:145–170.
- [3] Kandasamy R, Loganathan P, Arasu PP (2011) Scaling group transformation for MHD boundary layer flow of a nanofluid past a vertical stretching surface in the presence of suction and injection, Nuclear Eng Design, 241: 2053–2059.
- [4] Lin, C. R., and Shih, Y. P., “Laminar boundary layer heat transfer along static and moving cylinder”, J. Chin. Inst. Eng., vol. 3, 1980, pp. 73 –79.
- [5] Lin, C. R., and Shih, Y. P., “Buoyancy effects on the laminar boundary layer heat transfer along vertically moving cylinder”, J. Chin. Inst. Eng., vol. 4, 1981, pp. 45 – 51.
- [6] Wang, C. Y., “Fluid flow due to a stretching cylinder”, Phys Fluids. ,1988, 31: pp. 466–468.
- [7] Ishak, A., Nazar, R., Pop, I., “Magnetohydrodynamic (MHD) flow and heat transfer due to a stretching cylinder”, Energy Convers Manag ,2008, 49:pp. 3265 – 3269.
- [8] Elbashbeshy, E. M. A., Emam, T. G., El – Azab, M. S., Abdelgaber, K.M., “Laminar boundary layer flow along a stretching horizontal cylinder embedded in a porous medium in the presence of a heat source or sink with suction/injection”, International Journal of Energy & Technology ,2012, 4 (28) pp. 1 – 6.
- [9] R. Nazar, L. Tham, I. Pop, and D. Ingham, “Mixed convection boundary layer flow from a horizontal circular cylinder embedded in a porous medium filled with a nanofluid,” Transport in porous media, vol. 86, no. 2, pp. 517–536, 2011.
- [10] Srinivas Maripala and Kishan Naikoti, “Unsteady MHD flow and heat transfer of nanofluid over a permeable shrinking sheet with thermal radiation and chemical reaction” American Journal of Engineering Research, Volume-4, Issue-6, pp-68-79.
- [11] Brewster MQ (1992), Thermal radiative transfer properties, Wiley, New York, USA.



10.22214/IJRASET



45.98



IMPACT FACTOR:
7.129



IMPACT FACTOR:
7.429



INTERNATIONAL JOURNAL FOR RESEARCH

IN APPLIED SCIENCE & ENGINEERING TECHNOLOGY

Call : 08813907089  (24*7 Support on Whatsapp)